Lab on a Chip

RSC Publishing

PAPER

View Article Online
View Journal | View Issue

Active liquid degassing in microfluidic systems

Cite this: *Lab Chip*, 2013, **13**, 4366

J. Mikael Karlsson,[a] Muriel Gazin,[b] Sanna Laakso,[c] Tommy Haraldsson,*[a] Surbhi Malhotra-Kumar,[b] Minna Mäki,[d] Herman Goossens[b] and Wouter van der Wijngaart[a]

Received 27th June 2013,
Accepted 21st August 2013

DOI: 10.1039/c3lc50778e

www.rsc.org/loc

We present a method for efficient air bubble removal in microfluidic applications. Air bubbles are extracted from a liquid chamber into a vacuum chamber through a semipermeable membrane, consisting of PDMS coated with amorphous Teflon® AF 1600. Whereas air is efficiently extracted through the membrane, water loss is greatly reduced by the Teflon even at elevated temperatures. We present the water loss and permeability change with the amount of added Teflon AF to the membrane. Also, we demonstrate bubble-free, multiplex DNA amplification using PCR in a PDMS microfluidic device.

Introduction

The field of microfluidics constitutes an important step towards the next generation of diagnostic tools, fuel cells, medical devices, and synthesis and analysis of chemical and pharmacological compounds. A well-known reliability problem in microfluidics is the sensitivity to gas bubbles, which are formed in numerous ways. Trapping of air during liquid pumping is a common problem[1] and can lead to malfunctioning of devices *e.g.* by causing blockage of channels or sensor surfaces. There are also bubble-generating applications in which bubble removal is crucial for proper system function. Examples are cell culturing, where cytotoxic bubbles are formed,[2] and gas formation in fuel cells leading to barrier formation between the electrodes and liquid.[3] The device material itself has also been ascribed as a source of bubble formation in some cases.[1,4] Additionally, heating procedures *e.g.* thermal cell lysis, chemical molecular synthesis and DNA melting curve analysis, suffer from bubble formation through outgassing due to the reduced gas solubility at increased temperatures. Outgassing is a well-known cause of failure for on-chip polymerase chain reaction (PCR), since bubble formation leads to uneven heating and to expulsion of PCR mixture from the reaction chamber.[1,5]

Many different approaches to avoid bubble-generated problems have been previously described.[1–23] There are passive and active methods, and the main techniques used are bubble traps, bubble formation prevention methods, and bubble removal methods using pressurisation and/or extraction of bubbles, see Table 1. Bubble traps and multiphase flow systems function for certain applications,[6,7] but suffer from increased gas pressures at elevated temperatures, which may cause significant bubble expansions. Prevention of gas transport from the surroundings into microchannels using claddings[1] or barriers[4,8] have been shown to partly solve the problem of bubble formation in porous materials, though problems with bubble formation *via* trapping of large bubbles during liquid pumping and outgassing remain unsolved. Pressurisation of the system is an effective means to increase the gas solubility in liquids,[9,10] hence reducing bubble growth, though the high pressure requires sufficient interlayer bond strength of the device as well as stable valves.

The most popular approach for debubbling is based on extraction of gas from the microsystem *via* hydrophobic channels, pores or membranes (Table 1). Such approaches lead to higher debubbling reliability since the gas is partly or fully removed from the system, and are especially efficient in active systems where a pressure drop leads to gas transport through a membrane.[11,12]

Poly(dimethyl siloxane) (PDMS) is a commonly used material in rapid prototyping of microfluidic chips due to its ease of use and fabrication, compatibility with many biological and chemical processes and optical transparency. Also, a common approach for valving in lab-on-chip systems are based on pneumatic pinching, which requires an elastomeric material, such as PDMS.[24] In the field of membrane science, PDMS is extensively used due to its exceptionally high permeability to various gases and vapours, which can be attributed to its high free volume. This high permeability has led to

[a] *Micro and Nanosystems, KTH Royal Institute of Technology, Osquldas väg 10, 100 44 Stockholm, Sweden. E-mail: tommyhar@kth.se; Fax +46 (0)810 0858; Tel: +46 (0)8799059*
[b] *Laboratory of Medical Microbiology, Vaccine & Infectious Diseases Institute, Universiteit Antwerpen, Wilrijk 2610, Belgium*
[c] *Mobidiag, Tukholmankatu 8, 00290 Helsinki, Finland. E-mail: sanna.laakso@mobidiag.com; Fax: +358 9 191 25020; Tel: +358 9 191 25024*
[d] *Orion Diagnostica Oy, P.O. Box 83, 02101 Espoo, Finland. E-mail: minna.maki@oriondiagnostica.fi; Fax: +358 50 966 5837; Tel: +358 10 426 2794*

Table 1 Overview of bubble prevention methods previously described for microsystems

Authors	Passive debubbling	Active debubbling	Bubble trap	Merging of bubbles into gas pocket	Coating against microbubble formation	Gas barrier implant	Pressurisation to increase gas solubility	Bubble extraction	Gas extraction through microchannel	Gas extraction through open pores	Gas extraction through porous membrane	Gas extraction through PDMS	Temperature > 50 °C funtionality	Vapour loss control	Bubble gas	Liquid	Materials
Sung and Schuler[6]	X	-	X	-	-	-	-	-	-	-	-	-	-	-	Air, vapour	H_2O, culture medium	PDMS, glass
Hibara *et al.*[7]	X	-	-	X	-	-	-	-	-	-	-	-	-	-	O_2, N_2, vapour	H_2O	Glass
Chang *et al.*[16]	X	-	-	-	X	-	-	-	-	-	-	-	-	-	Air, vapour	H_2O	Glass, Teflon tape
Liu *et al.*[1]	X	-	-	-	X	-	-	-	-	-	-	-	X	-	Air, vapour	PCR mixture	PDMS, glass, cladding
Shin *et al.*[4]	X	-	-	-	-	X	-	-	-	-	-	-	X	X	Air, vapour	PCR mixture	PDMS, parylene coating
Ranjit Prakash *et al.*[8]	X	-	-	-	-	X	X	-	-	-	-	-	X	X	Air, vapour	PCR mixture	PDMS, glass, polyethylene
Nakayama *et al.*[9]	X	-	-	-	-	-	X	-	-	-	-	-	X	-	Air, vapour	PCR mixture	PDMS, glass, fluorinated oil
Wang *et al.*[10]	X	-	-	-	-	-	X	-	-	-	-	-	X	X	Air, vapour	PCR mixture	Polycarbonate, hydrogel
Metz *et al.*[17]	X	-	-	-	-	-	-	X	X	-	-	-	-	-	Air, vapour	H_2O	PDMS
Yang *et al.*[18]	X	-	-	-	-	-	-	X	X	-	-	-	-	-	Air, vapour	H_2O	Si, glass, PZT
Meng *et al.*[19]	X	-	-	-	-	-	-	X	-	X	-	-	-	-	CO_2, vapour	$NaHCO_3$, H_2SO_4	Si, glass, Teflon
Kamitani *et al.*[20]	X	-	-	-	-	-	-	X	-	-	X	-	-	-	CO_2, vapour	H_2O, CH_3OH	Si, glass, PDMS, membrane
Zheng *et al.*[21]	X	-	-	-	-	-	-	X	-	-	X	-	-	-	Air, vapour	Culture medium	PDMS, glass, filter
Liu *et al.*[22]	X	-	-	-	-	-	-	X	-	-	X	-	-	-	Air, vapour	H_2O, PBS	PMMA, PTFE membrane
Paust *et al.*[3]	X	-	-	-	-	-	-	X	-	-	X	-	-	-	CO_2, vapour	H_2O, CH_3OH	COC, PTFE membrane, more
Zhu[11]	-	X	-	-	-	-	-	X	-	-	X	-	-	-	Air, vapour	H_2O	Polyimide, membranes
Xu *et al.*[12]	-	X	-	-	-	-	-	X	-	-	X	-	-	-	Air, vapour	H_2O	PMMA, tape, membrane
Kang *et al.*[14]	-	X	-	-	-	-	-	X	-	-	-	X	-	-	Air, vapour	Culture medium	PDMS, glass
Eddings and Gale[13]	-	X	-	-	-	-	-	X	-	-	-	X	-	-	Air, vapour	H_2O, surfactant	PDMS
Johnson *et al.*[23]	-	X	-	-	-	-	-	X	-	-	-	X	-	-	Air, vapour	H_2O	Glass, tape, PDMS
Skelley and Voldman[2]	-	X	-	-	-	-	-	X	-	-	-	X	-	-	Air, vapour	H_2O	PDMS, glass, polystyrene
Lochovsky *et al.*[15]	-	X	-	-	-	-	-	X	-	-	-	X	-	-	Air, N_2, vapour	H_2O, CH_3CH_2OH	PDMS, glass
Liu et al.[1]	-	X	-	-	-	-	-	X	-	-	-	X	X	-	Air, vapour	PCR mixture	PDMS, glass
(This work)	-	X	-	-	-	-	-	X	-	-	-	X	X	X	Air, vapour	H_2O, PCR mixture	Si, PDMS, Teflon AF

problems with bubble formation in microfluidic systems, since air can readily enter through the PDMS into the on-chip liquid.[1,4] However, the high permeability to air has also been utilized to pump liquids into microchannels[13] and remove bubbles by either pressing bubbles from microfluidic channels into the PDMS[14] or by active suction through the polymer using an external vacuum source.[1,2,15] A common problem for all bubble extraction methods is loss of liquid during the extraction. PDMS-based debubbling systems suffer especially from water loss, since the polymer is considerably more permeable to water vapour than to air,[25] leading to significant loss of water in PDMS-based debubbling systems. Water loss is especially problematic for high-temperature applications, and has been observed as a source for failure in on-chip PCR.[8] The equilibrium vapour pressure increases rapidly with increasing temperature, and therefore, a large portion of the gas bubble.

Volume in aqueous solutions at elevated temperatures consists of vapour. A coating of the glassy copolymer Teflon Amorphous Fluoropolymer (Teflon AF) has been successfully used on carbon membranes to effectively reduce water transport while maintaining gas transport.[26] It has previously been shown that Teflon AF can be deposited on PDMS for use as cladding material in optical waveguides[27] and to reduce adhesion on moulds.[28]

Concept

Here we present the first bubble extraction method functional at high temperatures with low water loss, as can be seen in Table 1. In this work, we investigate and optimise the active extraction of bubbles through a semipermeable membrane (Fig. 1A), as previously presented by our group.[5,29] We combine the permeability of PDMS to extract gas bubbles with the barrier properties of Teflon AF to reduce water loss. The approach presented here relies on bubble transport from a microfluidic chamber through a membrane into a low-pressure chamber. This approach is suitable for degassing in integrated microfluidic systems, where only limited control of bubble formation by trapping and outgassing is achievable.

Experimental

Manufacturing approach

PDMS-based microfluidic cartridges (Fig. 1C–D), containing a top PDMS layer with a 10 μl vacuum chamber and a bottom

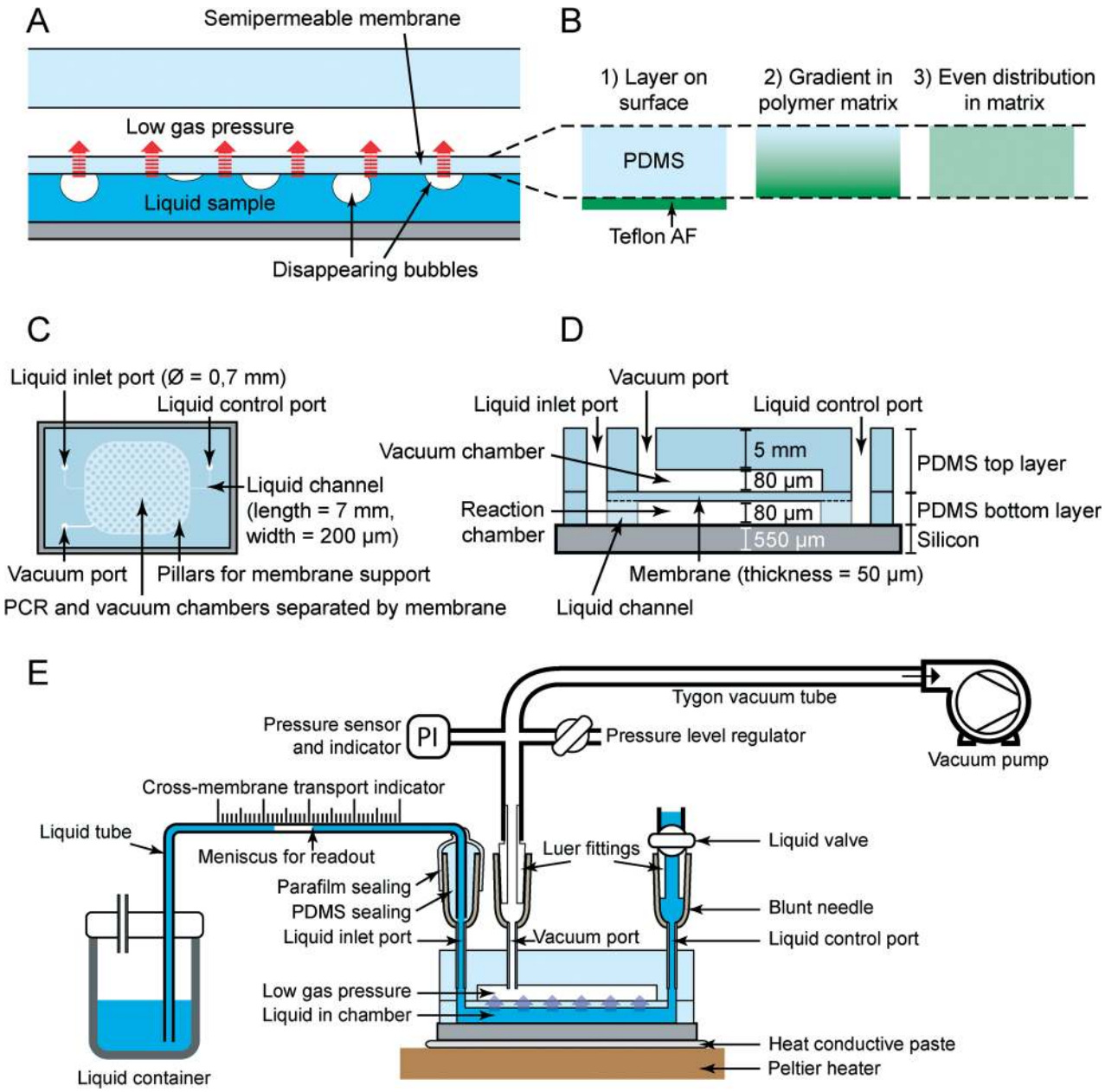

Fig. 1 (A) Debubbling principle, showing bubbles disappearing from a liquid-filled reaction chamber into a vacuum chamber. (B) Deposition of Teflon AF leads to three possible variants of Teflon distribution in PDMS. (C) Schematic top view and (D) cross-sectional side view showing dimensions of the microfluidic structure manufactured for permeability experiments. (E) Setup used for measurements of water loss through the semipermeable membrane.

PDMS layer with a 10 µl liquid chamber and a suspended membrane of 1.2 cm^2 area separating the two chambers were fabricated according to a previously described process.[5] The two-chamber structure features a liquid inlet port and a liquid control port connecting the liquid chamber, and a vacuum port connecting the vacuum chamber. For the PCR experiments, cartridges containing three sets of two-chamber structures, each containing a liquid chamber, a liquid inlet, a liquid control port, and a vacuum chamber, were used.

The Teflon AF coating of the membranes was performed as follows. Bottom PDMS layers, containing the membrane, were placed with the membrane side against a microscope glass slide. Xurography-patterned cleanroom blue-tape (SWT 20 +, Nitto Denko, Japan) was positioned on the PDMS surfaces around the membrane as a mask to the Teflon coating. The structure was placed in a spinner and approximately 50 µl of a solution with 0.15–0.5% (w/w) Teflon® AF 1600 (DuPont, USA) in fluorinated oil (FC-40, 3M, USA) was dispensed onto the membrane. Within seconds after dispensing the Teflon AF, spinning was initiated (1200 rpm, 60 s, 500 rpm s^{-1}). After spinning, the blue-tape was removed and the glass carrier with the PDMS structure was placed on a hotplate (175 °C, 15 min) to drive off the solvent. The process of masking, spin-coating and baking was repeated for the number of Teflon AF coatings

needed. Two reference structures were made according to the same recipe: a bottom PDMS layer coated with Teflon-free fluorinated oil, and a plain silicon wafer coated with 0.15% (w/w) Teflon AF in fluorinated oil. After completing the Teflon AF coating, the structures were assembled with a silicon substrate and a top PDMS layer, as previously described.[5]

Teflon deposition

We hypothesise that the deposition of Teflon AF/fluorinated oil onto a PDMS membrane results in a distribution profile of Teflon AF in the membrane according to one of three cases, illustrated in Fig 1B. Either the Teflon AF is deposited as a separate layer on the PDMS surface (1), or sorption of the fluorinated oil into the PDMS leads to a gradual (2) or an even (3) distribution of Teflon within the membrane. Investigation of the Teflon AF distribution in the membrane was performed in four steps. Firstly, swelling measurements of PDMS by fluorinated oil were performed by weighing a piece of PDMS before and after 24 hours immersion in FC-40. Secondly, ellipsometry measurements (UVISEL, Horiba) were performed (photon energy: 1.5–6.5 eV, Teflon AF refractive index: $n = 1.31$[27]) on bottom PDMS layers and plain silicon wafers, with one coating made from 0.15% (w/w) Teflon AF in oil. Thirdly, bottom PDMS layers were prepared with 0 and 5 coatings made from 0.15% (w/w) Teflon AF in oil. SEM-EDX (Ultra 55, Carl Zeiss; QUANTAX EDS, Bruker Nano GmbH) measurements (EHT 10 kV, WD 8.3 mm, 78 ×) of fluorine levels on both the coated and non-coated sides of the membranes were performed to see whether Teflon AF had diffused across the PDMS membranes. Lastly, permeability measurements were performed, as described in the following section.

Permeability investigation

Microfluidic test structures were fabricated, containing 0–6 coatings made from 0.15% (w/w) Teflon AF in oil as described above. These were investigated using a setup for water and air permeability measurements (Fig. 1E). The microchips were adhered to a hotplate using conductive paste, after which the temperature was raised to 95 °C. A vacuum pump was then coupled to the microchip vacuum chamber *via* a regulator and pressure sensor.

For the water loss experiments, a polyethylene tube with water was connected to the liquid inlet port. A container with deionised water was placed on a height-adjustable stage to ensure zero hydrostatic pressure. Water was pumped into the reaction chamber by the application of vacuum at the vacuum port, which led to water filling of the liquid chamber by evacuation of the air through the membrane. A small air bubble was introduced into the liquid tube as a tracer for volumetric flow through the membrane, and its movement along a position indicator was recorded with a camera.

Similarly, for the air permeability test, a tube was connected to the inlet port and air flow was recorded *via* the movement of a paraffin oil droplet (Jula, Sweden). Cross-membrane pressure drops of 90, 50, 25, 20 and 15 kPa were used in the permeability measurements. Also, an experiment at 72 °C and 90 kPa pressure drop was performed for a microchip with 5 Teflon coatings to investigate the temperature influence on permeability. After the experiments, the microchips were opened, and the membrane thicknesses were measured using microscopy.

Debubbling efficiency

Debubbling efficiency was investigated for two microchip designs with different Teflon coatings and sample liquids. First, a microchip with five Teflon coatings made from 0.15% (w/w) Teflon AF in oil was tested with filtered, deionised water. Second, a microchip with triplicate microfluidic chamber structures and membranes with coatings made from 0.5% (w/w) Teflon AF in oil, was tested with PCR sample, prepared according to the next section. Filling of liquid into the liquid chambers was performed by initiating degassing, as described in the section above. After priming, the vacuum port was coupled to atmospheric pressure, stopping the degassing. Thereafter, the temperature was increased to 96 °C, which caused gas bubbles to appear. When approximately 50% of the chamber volume was filled with gas, degassing was initiated using a 50 kPa cross-membrane pressure. Photographs of the liquid chamber were acquired every 10 s to monitor the amount of gas in the liquid chamber during the degassing. Image analysis was used on each photograph to measure the water/gas ratio in the chambers.

Multiplex PCR and hybridisation to DNA array

PCR experiments were performed in microchips containing triplicate microfluidic chamber structures and membranes, each with a single coating made from 0.5% (w/w) Teflon AF in oil. The chip was loaded into a holder of a Peltier-based thermocycler machine, controlled *via* software (Ana Light®, Farfield Group Ltd, UK). The DNA template used in the on-chip PCR experiments contained gene sequences unique for methicillin-resistant *Staphylococcus aureus* (MRSA, strain 2233/97). *S. aureus* specific primers (*nuc*, 200 bp) were combined with previously described[30] primers for detection of methicillin-resistant gene (*mecA*, 230 bp) thus enabling detection of MRSA.1.5 μl of isolated MRSA DNA (3.55×10^7 copies per microliter) was mixed with the PCR reaction mixture containing 0.125 μM of nucF primer (Metabion, Germany), 0.125 μM of biotin labelled nucR primer (Metabion, Germany), 0.125 μM of mecAF primer (Metabion, Germany), 0.125 μM biotin labelled mecAR primer (Metabion, Germany), 1× Hot Start Taq® PCR buffer (Qiagen, Germany), in which the final concentration $MgCl_2$ was 2.0 mM, 300 μM of each of dNTP (Finnzymes, Finland), 1.5 g l^{-1} BSA (EuroClone, Italy), 0.125 U μl^{-1} Hot Start Taq® DNA polymerase (Qiagen, Germany) and water to bring the total volume to 15 μl. The initial denaturation of 95 °C for 15 min was performed off-chip after which the PCR mixture was distributed to the six liquid ports on the microchip. Thereafter,

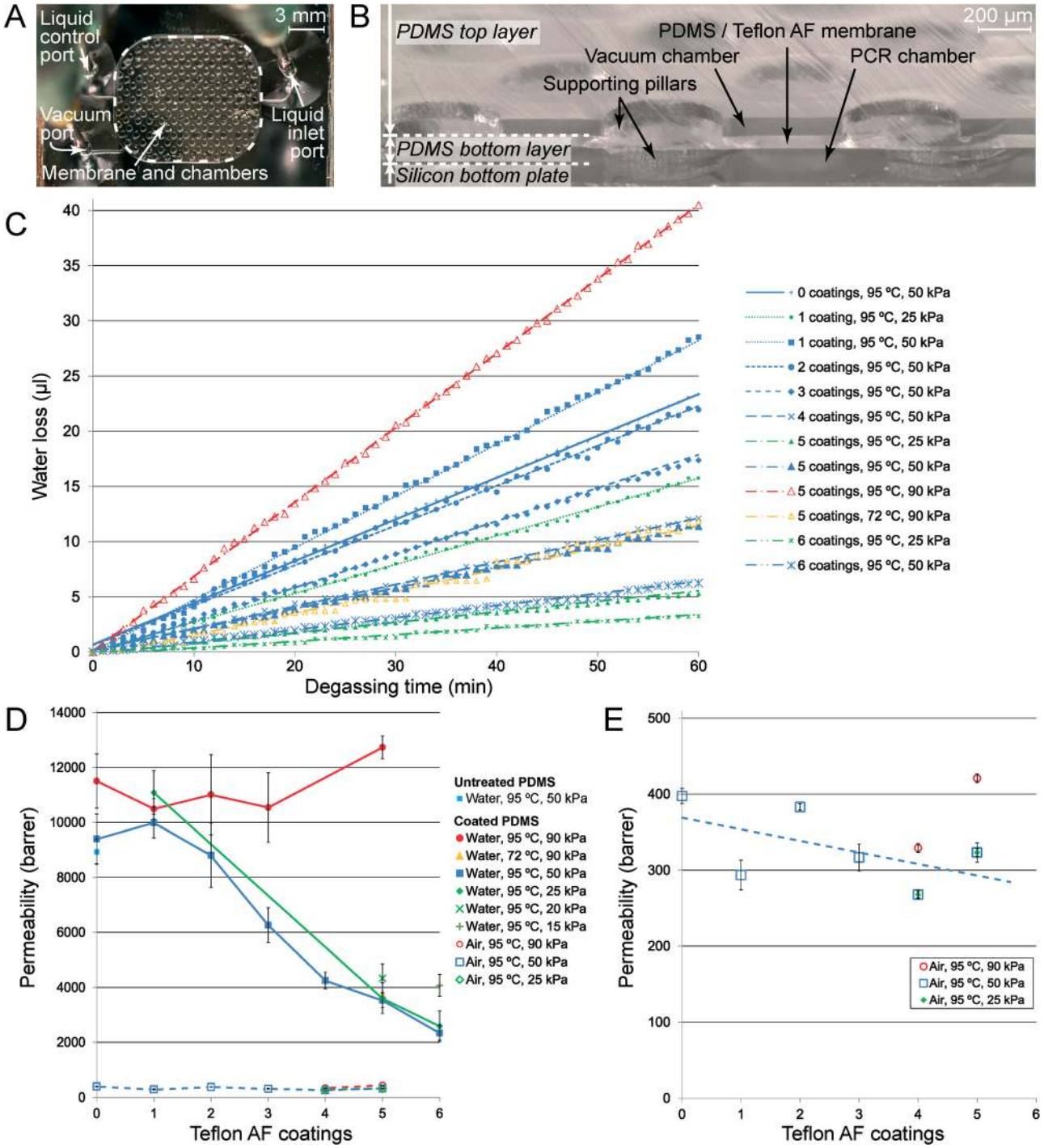

Fig. 2 (A) Top view photograph of manufactured microchip. (B) Microscope image of microchip cross-section for membrane thickness measurement. (C) Water loss during 1 h in microchips with membranes with different Teflon AF coatings. Least square linear fittings of data are indicated. (D) Permeability of water and air through PDMS membranes with increasing number of Teflon AF coatings, calculated from the data fitting in (C), with lines connecting the data points for eye guidance. (E) Detailed view over the air permeability from (D) with dotted line indicating linear curve fit to 50 kPa data.

50 kPa cross-membrane pressure drop was applied to initiate liquid priming of the chambers. After 1 min, all chambers were filled, and the thermocycling protocol (36 cycles of: 10 s at 96 °C, 35 s at 58 °C, 10 s at 72 °C, and final cooling down to 10 °C) was initiated. A reference PCR experiment was carried out using the same protocol in a Mastercycler® ep gradient S thermocycler (Eppendorf, Germany). After the PCR experiment, the PCR products were extracted *via* the liquid ports and analysed with a microarray (Prove-it™ TubeArray, Mobidiag, Finland) according to established protocols.[30,31] First, specific probes targeted for *nuc* and *mecA* genes were designed and printed on the microarray for hybridization.

Thereafter, the PCR amplicons were hybridised, whereafter the array was treated with horse radish peroxidase (HRP) and 3,3',5,5'-tetramethylbenzidine (TMB) to enable colorimetric detection of *S. aureus* and *mec A* methicillin resistant gene from the MRSA sample.

Results and discussion

Teflon deposition study

Swelling measurements showed a PDMS mass increase from 2.850 g to 2.866 g (*i.e.* 0.6%) from the Teflon AF solution treatment. This indicates that the Teflon AF solution is absorbed by the PDMS matrix. No results could be obtained from ellipsometry measurements of Teflon AF on PDMS, indicating that no clear interface between the PDMS and Teflon AF could be distinguished, possibly due to diffusion of Teflon AF into the PDMS matrix. Teflon AF deposited on the silicon reference substrate was measured to have a thickness of 8 nm using ellipsometry. SEM-EDX analysis of the deposition side of PDMS membranes with 5 layers of Teflon AF showed fluorine levels of 1–8% (w/w). EDX analysis on the non-coated side of the membranes showed traces of fluorine just above the noise level (<0.9%) on some of the sample points. The depth of the EDX interaction volume was at most a few micrometres. This indicates that traces of Teflon AF had diffused through the membrane, although most of the Teflon AF either remained on the deposition side as a layer (hypothesis 1, with a diffuse Teflon–PDMS boundary) or was distributed in a gradient inside the membrane (hypothesis 2).

Permeability and debubbling efficiency measurements

Microfluidic cartridges containing vacuum chambers, suspended membranes and PCR chambers were successfully manufactured (Fig. 2A) and membrane thicknesses were measured using microscopy (Fig. 2B) for calculation of permeability data. Readout from the images of the meniscus movements from the water loss and permeability measurements resulted in the graphs shown in Fig. 2C–E. A distinct correlation between the amount of Teflon AF coatings and the reduction in water loss was observed (Fig. 2D). Permeability dependence on the amount of Teflon coatings was calculated[25] for water and air at cross-membrane pressure drops of 90, 50, 25, 20 and 15 kPa (Fig. 2D and E). At 50 kPa pressure drop, the water permeability was significantly reduced with only few coatings of Teflon AF, whereas the air permeability showed no significant reduction with the number of Teflon AF coatings (Fig. 2D and E). Since lower pressure drops should result in lower water loss, it was of interest to test pressure drops of 25, 20 and 15 kPa, though no significant change was observed compared to 50 kPa. Operation at 72 °C resulted in water loss and permeability greatly reduced compared to operation at 95 °C, which implies that the water loss expected from thermocycling PCR experiments are lower than the results in Fig. 2C. The difference in water permeability between the untreated PDMS (9700 barrer) and the PDMS with the Teflon-free fluorinated oil treatment (10 100 barrer) was insignificant, indicating that the water loss reduction in the experiments can be attributed to the Teflon AF layer depositions.

It can be seen in Fig. 2D that a significant increase in water vapour transmission was recorded when the cross-membrane pressure drop was increased from 50 to 90 kPa, resulting in permeability values comparable to uncoated PDMS. Whereas permeability of water through PDMS is affected by the upstream water vapour pressure,[32] it is unlikely that a lowered downstream pressure will increase water permeability through our Teflon-coated PDMS membrane to the extent observed in Fig. 2D. However, the elastomeric membrane deforms increasingly with increasing pressure difference. We speculate that the deformation causes formation and expansion of cracks in a glassy layer of

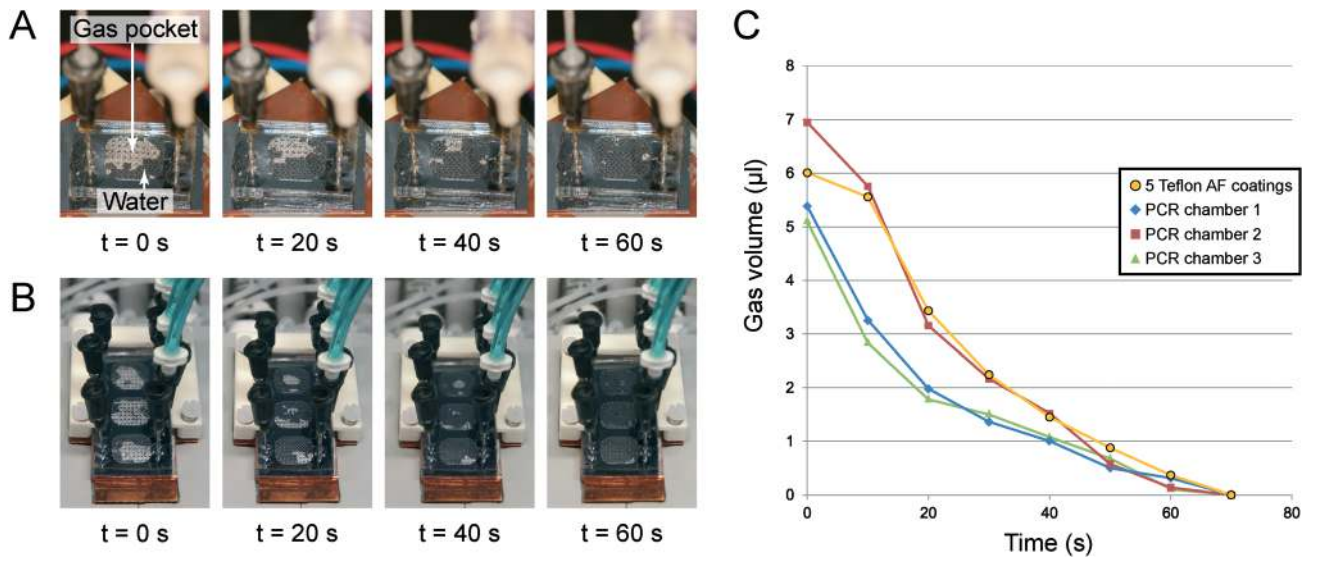

Fig. 3 Degassing efficiency at 50 kPa cross-membrane pressure drop in (A) a water-filled microchip with 5 coatings of Teflon and (B) a PCR reaction mixture-filled microchip with three individual chambers with membranes. (C) The debubbling efficiency obtained using image analysis on photographs from the measurements.

Teflon AF on the membrane, thus exposing highly permeable PDMS. The permeability increase at 90 kPa was observed to be reversible by decreasing the pressure drop to 50 kPa (results not shown). Although these observations suggest that the water-repellent properties result from a layer-like coating of Teflon AF on the PDMS surface, further investigations are required to fully understand the Teflon AF distribution and what interactions between the membrane and water molecules this results in.

Debubbling efficiency

Degassing of water and PCR mixture in the two microchip designs resulted in efficiencies as shown in Fig. 3. In both cases, gas-free microchip chambers were obtained after approximately 70 s of continuous degassing. The reduced gas removal rate with time, which can be observed as the time derivative of the curves shown in Fig. 3C, is caused by the reduced membrane area in contact with gas as the gas pocket volume decreases. The high debubbling efficiency (Fig. 3C) and the low reduction of air permeability by added Teflon AF layers observed (Fig. 2E) indicate that a thicker Teflon AF coating than used here has the ability to provide even lower water loss and still enable air bubble removal.

Multiplex on-chip PCR with debubbling

The DNA array readouts show successful hybridisation of both *nuc* and *mec A* amplicons (Fig. 4A and B), perfectly matching the readout of MRSA on our microarray. This shows that the multiplex PCR was successful in microchips with debubbling functionality. Debubbling was efficient during the PCR experiments, though occasionally small bubbles were observed. Since the PCR sample was thermocycled (Fig. 4C), it was only exposed to 96 °C for 10 s per cycle, whereafter the temperature was lowered to 58 °C. Therefore, bubbles that did not have time to cross the membrane rapidly, dissolved into the PCR mixture during low temperature. Permeability increases exponentially with temperature,[25] and as shown previously,[29] water loss is considerably reduced during thermocycling as compared to static exposure at 96 °C, which agrees with the results in Fig. 2C. A feature of this bubble removal approach is that PDMS prevents transport of large molecules, thus largely reducing the risk of contaminating the environment with amplicons,

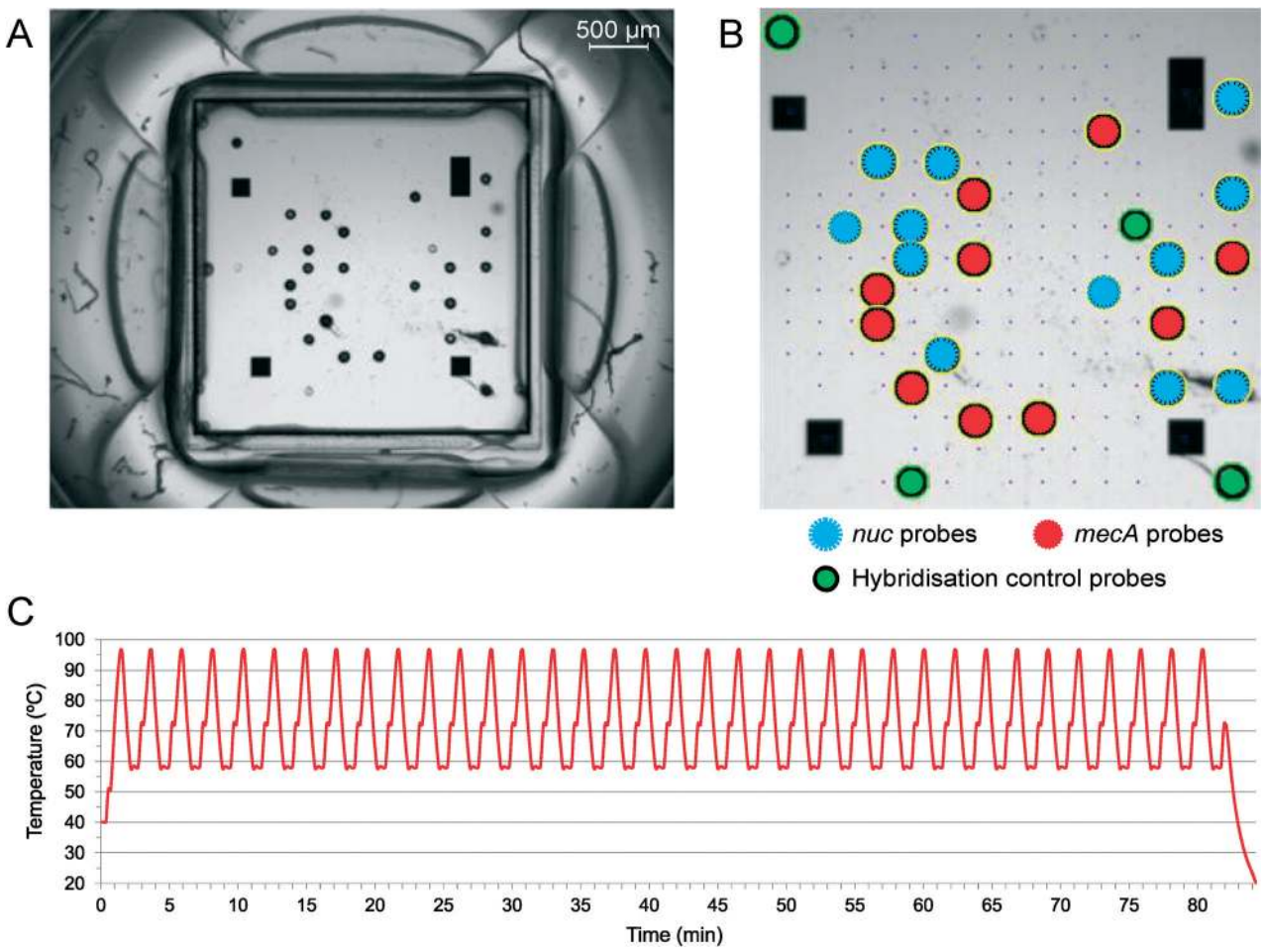

Fig. 4 MRSA detection of PCR product extracted from microchips using degassing. (A) Microscope photograph of the DNA array, showing successful hybridisation at sites with dark spots. (B) Analysed array image obtained from the Prove-it™ software, showing successful hybridisation at spots with *nuc*, *mecA* and hybridisation control probes.

in contrast to debubbling methods using open pores. From the results presented here, we conclude that the debubbling method described in this work is highly efficient, effectively reduces water loss, and is suitable for on-chip PCR.

Conclusions

We show a novel approach for efficient gas bubble removal at high temperatures with only limited water loss using a pressure drop over a micromoulded PDMS membrane treated with Teflon AF 1600. The debubbling method does not require high pressures, bubble traps, or integration of blocking structures, and can be performed continuously during operation of the microfluidic device. Of high importance is a significant reduction of water permeability obtained by the addition of Teflon AF to the membrane. Successful bubble-free amplification and detection of MRSA was performed in a PDMS-based microchip using a multiplex PCR protocol and hybridisation to a DNA microarray. The method allows microfluidic systems to remain bubble-free and unaffected by water loss problems and is therefore highly suitable for liquid handling in total analysis microsystems.

Acknowledgements

This work has been financially supported by the European Union through the FP7 and IMI sponsored projects INTOPSENS and Rapp-ID.

References

1 H.-B. Liu, H.-Q. Gong, N. Ramalingam, Y. Jiang, C. C. Dai and K. M. Hu, *J. Micromech. Microeng.*, 2007, **17**, 2055–2064.
2 A. Skelley and J. Voldman, *Lab Chip*, 2008, **8**, 1733–1737.
3 N. Paust, S. Krumbholz, S. Munt, C. Müller, P. Koltay, R. Zengerle and C. Ziegler, *J. Power Sources*, 2009, **192**, 442–450.
4 Y. S. Shin, K. Cho, S. H. Lim, S. Chung, S.-J. Park, C. Chung, D.-C. Han and J. K. Chang, *J. Micromech. Microeng.*, 2003, **13**, 768.
5 J. M. Karlsson, T. Haraldsson, S. Laakso, A. Virtanen, M. Maki, G. Ronan and W. van der Wijngaart, in, *Solid-State Sensors, Actuators and Microsystems Conference (TRANSDUCERS), 2011 16th International*, 2011, pp. 22152218.
6 J. H. Sung and M. L. Shuler, *Biomed. Microdevices*, 2009, **11**, 731–738.
7 A. Hibara, S. Iwayama, S. Matsuoka, M. Ueno, Y. Kikutani, M. Tokeshi and T. Kitamori, *Anal. Chem.*, 2005, **77**, 943–947.
8 A. Ranjit Prakash, S. Adamia, V. Sieben, P. Pilarski, L. M. Pilarski and C. J. Backhouse, *Sens. Actuators, B*, 2006, **113**, 398–409.
9 T. Nakayama, Y. Kurosawa, S. Furui, K. Kerman, M. Kobayashi, S. R. Rao, Y. Yonezawa, K. Nakano, A. Hino, S. Yamamura, Y. Takamura and E. Tamiya, *Anal. Bioanal. Chem.*, 2006, **386**, 1327–1333.
10 J. Wang, Z. Chen, M. Mauk, K.-S. Hong, M. Li, S. Yang and H. H. Bau, *Biomed. Microdevices*, 2005, **7**, 313–322.
11 X. Zhu, *Microsyst. Technol.*, 2009, **15**, 1459–1465.
12 J. Xu, R. Vaillant and D. Attinger, *Microfluid. Nanofluid.*, 2010, **9**, 765–772.
13 M. A. Eddings and B. K. Gale, *J. Micromech. Microeng.*, 2006, **16**, 2396–2402.
14 J. H. Kang, Y. C. Kim and J.-K. Park, *Lab Chip*, 2008, **8**, 176.
15 C. Lochovsky, S. Yasotharan and A. Günther, *Lab Chip*, 2012, **12**, 595–601.
16 F.-M. Chang, Y.-J. Sheng, S.-L. Cheng and H.-K. Tsao, *Appl. Phys. Lett.*, 2008, **92**, 264102.
17 T. Metz, W. Streule, R. Zengerle and P. Koltay, *Langmuir*, 2008, **24**, 9204–9206.
18 Z. Yang, S. Matsumoto and R. Maeda, *Sens. Actuators, A*, 2002, **95**, 274–280.
19 D. D. Meng, J. Kim and C.-J. Kim, *J. Micromech. Microeng.*, 2006, **16**, 419.
20 A. Kamitani, S. Morishita, H. Kotaki and S. Arscott, *J. Power Sources*, 2009, **187**, 148–155.
21 W. Zheng, Z. Wang, W. Zhang and X. Jiang, *Lab Chip*, 2010, **10**, 2906.
22 C. Liu, J. A. Thompson and H. H. Bau, *Lab Chip*, 2011, **11**, 1688–1693.
23 M. Johnson, G. Liddiard, M. Eddings and B. Gale, *J. Micromech. Microeng.*, 2009, **19**, 095011.
24 M. A. Unger, H. P. Chou, T. Thorsen, A. Scherer and S. R. Quake, *Science*, 2000, **288**, 113–116.
25 S. Matteucci, Y. Yampolskii, B. D. Freeman and I. Pinnau, *Mater. Sci. Membr. Gas Vap. Sep.*, 2006, 1–49.
26 C. W. Jones and W. J. Koros, *Ind. Eng. Chem. Res.*, 1995, **34**, 164–167.
27 S. H. Cho, J. Godin and Y.-H. Lo, *IEEE Photonics Technol. Lett.*, 2009, **21**, 1057–1059.
28 W. M. Choi and O. O. Park, *Microelectron. Eng.*, 2003, **70**, 131–136.
29 J. M. Karlsson, T. Haraldsson, N. Sandström, G. Stemme, A. Russom and W. van der Wijngaart in, *Proceedings Micro Total Analysis Systems (μTAS) 2010*, 2010, pp. 17901792.
30 A.-K. Järvinen, S. Laakso, P. Piiparinen, A. Aittakorpi, M. Lindfors, L. Huopaniemi, H. Piiparinen and M. Mäki, *BMC Microbiol.*, 2009, **9**, 161.
31 P. Tissari, A. Zumla, E. Tarkka, S. Mero, L. Savolainen, M. Vaara, A. Aittakorpi, S. Laakso, M. Lindfors, H. Piiparinen, M. Mäki, C. Carder, J. Huggett and V. Gant, *Lancet*, **16**(375), 224–230.
32 S. J. Harley, E. A. Glascoe and R. S. Maxwell, *J. Phys. Chem. B*, 2012, **116**, 14183–14190.